Tropical Cyclone Hazard Assessment Using Model-based Track Simulation

Jonas Rumpf[1*]**, Helga Weindl**[2]**, Peter Höppe**[2]**, Ernst Rauch**[2]**,
Volker Schmidt**[1]

[1] Ulm University, Institute of Stochastics, 89069 Ulm, Germany
[2] Munich Reinsurance Company, 80791 Munich, Germany

Abstract A method is introduced for assessing the probabilities and intensities of tropical cyclones at landfall and applied to data from the North Atlantic. First, a recently developed model for the basin-wide Monte-Carlo simulation of tropical cyclone tracks is enhanced and transferred to the North Atlantic basin. Subsequently, a large number of synthetic tracks is generated by means of an implementation of this model. This synthetic data is far more comprehensive than the available historical data, whilst exhibiting the same basic characteristics. It thus creates a more sound basis for assessing landfall probabilities than previously available, especially in areas with a low historical landfall frequency.

Key words   tropical cyclones, hurricanes, landfall hazard, stochastic model, Monte-Carlo simulation

1 Introduction

1.1 Motivation

Tropical cyclones cause by far the highest losses for the insurance industry. In 2005, insured losses caused by North Atlantic cyclones exceeded US\$83bn, breaking all previous records for a single year (see Munich Reinsurance Company (2006), p.18). It is therefore necessary for insurance and reinsurance companies to assess these risks thoroughly and carefully. Unfortunately, the data available for risk assessment is relatively limited, covering (in the case of the North Atlantic) a time span of about 150 years, whereas

---

⋆ *Corresponding Author Address:* Jonas Rumpf, Ulm University, Institute of Stochastics, D-89069 Ulm, Germany; e-mail: `jonas.rumpf@uni-ulm.de`

reinsurers need to include wind speeds with much lower exceedance frequencies (< 0.001 p. a.) in their calculations. The approach to the solution of this problem taken in this paper is to enhance the stochastic model of tropical cyclone tracks in the western North Pacific originally introduced in Rumpf et al. (2006) and Rumpf et al. (2007) and then to apply it to the historical data on the North Atlantic basin. From this model, a number of synthetic but realistic storm tracks can be simulated that is much larger than the number of storms provided by the historical data. Since these synthetic tracks exhibit the same basic characteristics as the tracks observed in the past, they can be used to perform the calculations necessary for a more sound risk assessment. For example, the frequencies and return periods of wind speeds at certain points of interest can be calculated on the basis of a much larger dataset. It should be emphasized that the methods described in this study aim to reflect the characteristics of the historical data in their entirety, while the effects of potential fluctuations in cyclone activity are deliberately neglected for now. Influences such as the El Niño-Southern Oscillation (ENSO), North Atlantic Oscillation (NAO), or the Atlantic Multidecadal Oscillation (AMO) are 'averaged out' by pooling all available data regardless of the phases it occurred in.

The procedure for the simulation of tropical cyclone tracks can be outlined as follows: After simulating a point of genesis from an inhomogeneous Poisson point process model, the initial segment of a cyclone track is generated by sampling from the historically observed initial directions, initial translational speeds and initial wind speeds of cyclones starting in the vicinity of this genesis point. With this segment, a new position for the simulated cyclone track can be found. At the new position, changes in direction, translational speed, and wind speed are simulated, again by sampling from the historically observed values of these characteristics in the vicinity of the current position. In this way, a new segment for the cyclone track is constructed. Further segments are then simulated in the same way until it is decided to terminate the track. The random decision whether or not a track is terminated is made after each segment with a termination probability that is found as a function of the cyclone's current wind speed and position. The details of this simulation procedure are explained in Rumpf et al. (2006) and in part in Section 2.

For an overview of the statistical aspects of the modelling and analysis of losses caused by hurricanes, the reader is referred to the article by Iman et al. (2006) and the references it contains.

1.2 Overview

The first step involves presenting the data on which the model is based. The various components of the stochastic track model are then explained

in Section 2. This focuses in particular on the calculation of wind speeds
at certain distances from the simulated tracks (see Section 2.5). The meth-
ods of hazard assessment applied to the simulation results are described
in Section 3. Section 4 presents the results of simulations carried out with
an implementation of the model, and evaluates them in comparison to the
historical data. The summary in Section 5 rounds off the paper.

1.3 Data

The data used in this study are taken from the HURDAT best track data
(see Jarvinen et al. (1984)) provided by the National Oceanographic and
Atmospheric Administration of the United States of America (NOAA). Al-
though the database contains storms dating back to 1851, only the records
for the 1900-2005 period are used, older data being of doubtful reliability.
This complies with meteorological standard M-1 of the Florida Commission
on Hurricane Loss Projection Methodology (FCHLPM).

The information in HURDAT that is relevant to the proposed model
indicates the position and wind speed of each storm, recorded at regular
six-hour intervals. In this way, a cyclone track can be represented as a
polygonal trajectory that connects up to 132 points of storm measurement.
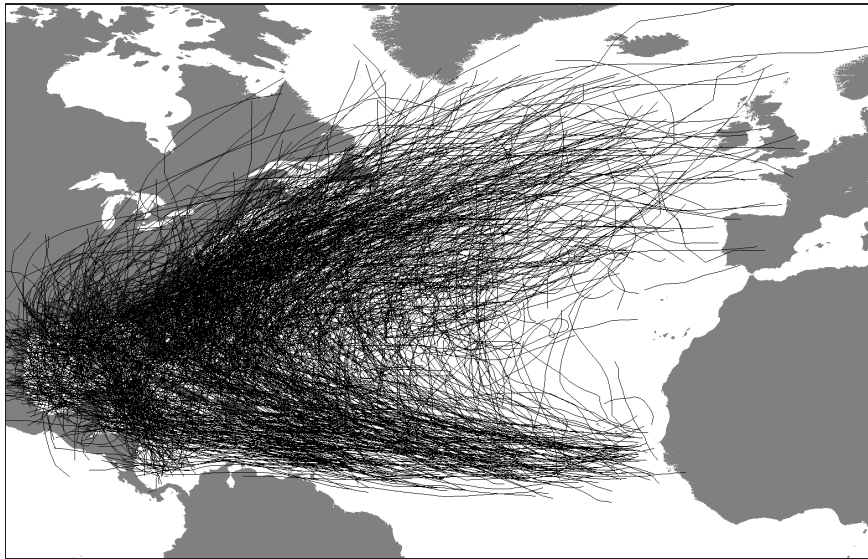The tracks of all 979 storms considered are plotted in Figure 1.

Figure 1 Tracks of all storms contained in the historical dataset

2 Stochastic track model

This section outlines the stochastic model used to simulate the tracks of
tropical cyclones. The basis for this model was first introduced in Rumpf et
al. (2006) and has been described in detail in Rumpf et al. (2007). Therefore,
only those parts of the model that constitute significant enhancements to
the original model are described at length, see for example Section 2.5. The
reader is referred to Rumpf et al. (2007) for details on other aspects of the
model.

2.1 Classification

It is obvious from Figure 1 that the cyclone track shapes exhibit strong in-
homogeneities. Therefore, as an auxiliary tool for simulating cyclone tracks,
the historical tracks are first split into six disjoint classes based on the loca-
tions of their starting and end points and the regions affected by the storms.
The track shapes in the respective classes are much more homogeneous, and
yield greater precision when the simulations are generated. Figures 5 and 7
show two examples of the resulting classes: class 1 storms (Figure 5) have a
relatively straight track from the open Atlantic into the Caribbean and the
Gulf of Mexico, whereas class 2 storms (Figure 7) initially take a similar
direction but then recurve towards the northeast, in most cases affecting
not only the Caribbean and/or the Gulf of Mexico but also Florida or some
other part of the eastern North American continent. The subsequent steps
in the modelling process are performed separately for the different classes,
making use of the improved homogeneity created by dividing the tracks into
classes.

2.2 Points of genesis

The first step in modelling the tracks of tropical cyclones is to describe the
points of cyclone genesis by means of a random point process model (see,
for example, Baddeley et al. (2006) and Diggle (2003)). In our case, it is ap-
propriate to employ a Poisson process model, due to the nature of the data.
A Poisson point process can be considered as a model for 'complete spatial
randomness', i.e. the points are placed independently of each other, while
their total number is Poisson distributed (see Stoyan and Stoyan (1994)).
This model therefore reflects the apparent absence of 'interaction' between
the starting points of cyclones in the historical data for the time period
1900-2005, a meteorological property that is also backed by the results of a
mathematical investigation into the point patterns of these points of gene-
sis. In this investigation, the frequencies of interpoint distances were plotted
to establish whether any attraction or repulsion effects between the points
of genesis were visible. These plots seemed to indicate only a minor degree
of interaction, if any. In consequence, further investigations were carried

out. Various point process models such as the Strauss hard core model were fitted to the data using `spatstat` (see Baddeley and Turner (2005)). The resulting model parameters did not indicate any relevant interaction between the points.

Furthermore, the point process model of which the points of cyclone genesis are considered a realisation is presumed to be spatially inhomogeneous, i.e. its intensity varies spatially. Figure 2 plots the points of genesis for historical class 2 storms to illustrate this assumption. The intensity function of the inhomogeneous Poisson process has to be estimated from the data in order to complete the model of the starting points of the cyclone tracks. This is done by means of a generalised nearest neighbour estimator (see Rumpf et al. (2007)), which uses an estimation technique closely related to kernel estimation. For details of the corresponding definition and properties, see Silverman (1986), p.97.

Figure 2 Points of genesis of class 2 storm tracks in the historical data

2.3 Cyclone tracks and wind speeds

As mentioned in Section 1.3, cyclone tracks can be interpreted as polygonal trajectories or as a sequence of track segments connecting the locations of measurement. Each track segment is uniquely determined by its starting point, orientation and length. Thus, storm tracks are modelled as a sequence of random vectors $S^{(i)} = \left(X^{(i)}, Y^{(i)}, Z^{(i)} \right)^{\top}$ in the following way:

the direction of storm movement (or orientation) $X^{(i+1)}$ along the $(i+1)$-th segment is interpreted as the state of a generalised random walk after the $(i+1)$-th step, i.e. as the sum of an initial direction X_0 and the subsequent independent changes in direction after the j-th segment, $X_j, 1 \leq j \leq i$:

$$X^{(i+1)} = \sum_{j=0}^{i} X_j \tag{1}$$

The distributions of X_0 and $X_j, j \geq 1$ are assumed to depend on the storm's current position, i.e. the endpoint of what is currently the last segment of the storm track. This approach relies on the same basic assumption as the track simulation models proposed for example in Emanuel et al. (2006) and Hall and Jewson (2007), namely that tropical cyclones with similar geographical positions behave in comparable ways due to similarities in their meteorological and geographical circumstances. In the model, this assumption is reflected by the fact that the distributions of X_0 and X_j are created by resampling from the historical data measured near the storm's current position.

Since the historical measurements have been taken at regular six-hour intervals, the length of a segment is more naturally modelled by finding the storm's translational speed along that segment and multiplying it by the duration of the interval. The model for translational speed Y, in turn, is then constructed in the same way as the one for X explained above, with the same dependence on the cyclone's current position. Note that while the current translational speed is seen as the sum of the initial speed and changes in that speed after each segment, it can not formally be considered a generalised random walk. Certain boundary conditions that have to be imposed on Y (most notably $Y \geq 0$) effectively make its changes a Markov process, i.e. a stochastic process whose probability distribution of the next state depends only on its current state but not on the past. For mathematically more rigorous treatments of Markov processes, see, for example, Meyn and Tweedie (1993) or Stroock (2005) and the references therein.

For a meaningful assessment of tropical cyclone hazards, it is also necessary to consider the maximum wind speeds Z along the cyclone tracks. In a similar way to that described above, the maximum wind speed $Z^{(i+1)}$ along the $(i+1)$-th segment is regarded as the sum of an initial wind speed Z_0 and the subsequent changes in wind speed Z_j after the j-th segment, $1 \leq j \leq i$. Again, the wind speed is not a generalised random walk. The changes in it have to be considered a Markov process, because besides some boundary conditions, the distribution of Z_j depends not only on the storm's current position (analogously to X_j and Y_j) but also on the previous wind speed $Z^{(j)}$. This latter dependence is introduced into the model to reflect a property of tropical cyclones observed in the data. For example, storms that reach very high wind speeds exhibit a tendency to weaken because there is

a high probability that they have reached their peak intensity. On the other hand, storms with low wind speeds could be in the early stages of their life cycle and still developing, or already close to the end of their track, and therefore of reducing intensity. To differentiate between these two possibilities, a location dependence of the changes in wind speed Z_j is constructed in complete analogy to the location dependence of the distributions of X_j and Y_j, because the main regions of cyclone genesis and of the termination of cyclones are different.

2.4 Termination probabilities

The termination of cyclone tracks is also described stochastically. As mentioned above, a basic underlying assumption of the whole model is that storms with similar positions behave in similar ways. It is therefore plausible to make the termination probability of a cyclone location-dependent, since the weakening and dissipation of a cyclone is strongly related to the influx of energy from warm water at its current position – or rather the lack thereof. On the other hand, the termination probability also has to depend on the current maximum wind speed of the storm, since a storm with a low wind speed is obviously much more likely to fall below the speed threshold of being a tropical storm during the subsequent 6 hours than a storm with a high wind speed.

Therefore, termination probability is calculated as being the maximum of a location-dependent and a wind-speed-dependent probability. Whilst the former is obtained as the relative frequency of termination points in the vicinity of the cyclone's current position, the latter is determined by fitting a curve to the historical termination probabilities as a function of the cyclone's current wind speed.

2.5 Radii and shapes of cyclones

The information incorporated into the model for the tracks of tropical cyclones so far has been limited to the polygonal trajectories, i.e. no statements are made about the situation outside the points of measurement and the segments connecting them. A real tropical cyclone, however, causes high wind speeds not only at its centre but also at locations a significant distance from the centre. It is therefore necessary to include information about the radius and the shape of the storms in the model. The proposed model does so in the following way: a tropical cyclone is considered to be a modified Rankine vortex of the form

$$v(r) = \begin{cases} v_{max} \cdot \frac{r}{r_{max}} & \text{if } 0 \leq r < r_{max} \ , \\ v_{max} \cdot \left(\frac{r}{r_{max}} \right)^{-x} & \text{if } r \geq r_{max} \ , \end{cases} \qquad (2)$$

where the wind speed $v(r)$ (in km/h) at a distance r from the centre is given as a function of r, of the radius r_{max} at which the maximum wind speed is attained, and of the maximum wind speed v_{max} (in km/h) itself for some $x \in [0, 1]$ (see, for example, Holland (1980)). The exponent x determines the shape of the wind profile, i.e. how quickly wind speed decreases with increasing distance outside of the radius of maximum wind speed. The value of x has to be found empirically. Reflecting the approach of the proposed model more naturally than determining x directly, is to determine the radius of maximum wind speed r_{max} and the gale-force radius r_{gale}. The gale-force radius r_{gale} is defined as the maximum distance from the centre of the storm at which wind speeds of at least gale force, i.e. $v_{gale} = 63$ km/h, are attained. Naturally, v_{max} is always assumed to be greater than v_{gale} (which also implies $r_{max} < r_{gale}$), since storms that do not attain wind speeds above gale force are not considered tropical storms (note that the data still contains measurements of maximum wind speeds below 63 km/h, mainly due to the possibility that a cyclone will regain strength after falling below r_{gale}, but also in part due to a number of data maintenance inconsistencies). In this way, the value of x can be determined using (2), if r_{max} and r_{gale} are known:

$$x = \frac{\ln(v_{max}) - \ln(63)}{\ln(r_{gale}) - \ln(r_{max})} \qquad (3)$$

Unfortunately, the data available on these radii constitute only a small fraction of the total measurements in HURDAT: The 'extended best track data' (see Demuth et al. (2006)) contains 225 storms with measurements of the radius of maximum wind speeds and the gale-force radius. This makes up approximately 23% of the best track HURDAT data used for this study (see Section 1.3). However, r_{max} and r_{gale} have not been recorded at all the measurement points of these storms. Thus, the total number of measurements with a recorded radius of maximum wind speed is reduced to approximately 15% of the HURDAT data measurements. This makes it inappropriate to deal with them as Markov processes with location-dependent distributions of the summands in analogy to the maximum wind speed. Instead, r_{max} and r_{gale} are calculated as empirical functions of the wind speed by exponential regression of $\frac{v_{max}}{r_{max}}$ and logarithmic regression of r_{gale}, respectively:

$$r_{max} = \frac{v_{max}}{a \cdot \exp(b\, v_{max})} \qquad (4)$$

$$r_{gale} = c \cdot \ln(v_{max}) - d \qquad (5)$$

The coefficients a, b, c, d are determined separately by least-squares regression for three different categories of cyclones: those who reach wind speeds of at least 210 km/h along their track, those whose highest wind speed along the track is between 140 km/h and 210 km/h, and those whose wind speeds never exceed 140 km/h, or in other words, strong, medium and weak cyclones. For any cyclone track simulated as described in Sections 2.2 to 2.4, r_{max} and r_{gale} at each point of measurement are then calculated as

functions (4) and (5) of v_{max}, for the values of a, b, c, d corresponding to the highest wind speed attained along the respective tracks. These functions can then be used to determine the value of x via (3).

In general, maximum wind speeds are measured on the right hand side of a storm, since the translation speed on that side adds to the tangential wind speeds. To take account of this fact, the translation speed (multiplied by the sine of the angle between storm direction and direction to the respective location) is subtracted from the wind speeds calculated from (2) for locations on the left-hand side of a storm.

Figure 3 shows a plot of the fitted exponential regression curves from (4) for the data available on the radii of maximum wind speeds r_{max}. An analogous graph is plotted in Figure 4 for the regression curves resulting from (5). Only the relevant parts of the curves are plotted; for values not included in the plot, the curves are either undistinguishable or not applicable, because the respective maximum wind speeds for the different categories of cyclones are exceeded.

3 Hazard assessment

As mentioned in Section 1.1, the stochastic track model described in this paper was developed in order to improve hazard assessment for areas affected by tropical cyclones. To this end, firstly a large number of synthetic storm tracks is generated from the implementation of the model. For example, a random Poisson distributed number (see Section 2.2) with an expectation $\frac{10,000}{106}$ times the number of historical tracks in the data considered (see Section 1.3) would represent the number of storms occuring over a time span of $m = 10,000$ years. As described above, each of these storms consists of several segments connecting the points of measurement. To calculate the cyclone hazard at a point of interest t_0 in the observation window, for each storm, the distance of t_0 to all points of measurement of this storm is calculated. The wind speeds with which t_0 is affected by the cyclone from its various positions can be determined by inserting these distances into (2). The maximum of all the wind speeds caused by a storm is then taken as the storm's 'wind impact' on t_0. By calculating the impacts of all simulated storms on t_0 for the time span of m years, a large number n_{t_0} of wind speeds is obtained, even if wind speeds of less than v_{gale} are discarded. Finally, the expected return period of any given wind speed v_0 can easily be estimated from those wind speeds by dividing the number of years m by the number of impacts on t_0 greater than or equal to v_0. Note that this method may produce the same estimate for the expected return period for different wind speeds. To obtain a one-to-one relation, a strictly monotonic parametric distribution function $F(v)$ (e. g. Gamma-, Weibull- or other extreme value distributions) could be fitted to the impacts calculated. Then the estimate
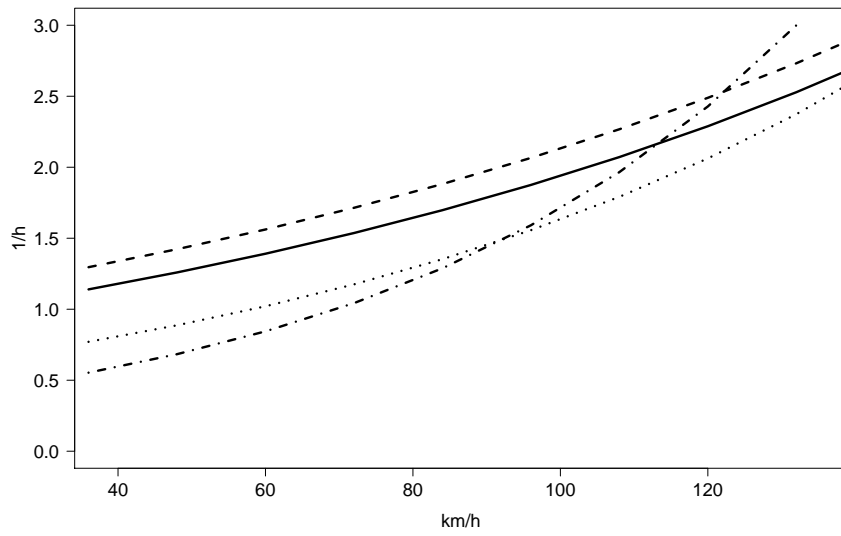
Figure 3 Exponential regression of $\frac{r_{max}}{v_{max}}$ as a function of v_{max}. Solid line: all cyclones; dashed line: strong cyclones; dotted line: medium cyclones; dot-dashed line: weak cyclones.

Figure 4 Logarithmic regression of r_{gale} as a function of v_{max}. Solid line: all cyclones; dashed line: strong cyclones; dotted line: medium cyclones; dot-dashed line: weak cyclones.
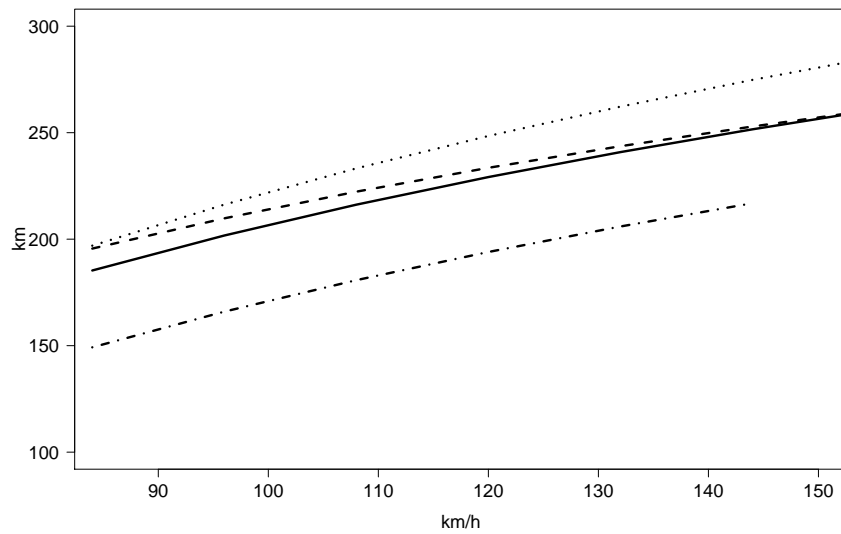
$\widehat{RP}(v_0)$ for the expected return period of v_0 could be calculated as

$$\widehat{RP}(v_0) = \frac{m}{n_{t_0}(1 - F(v_0))} \qquad (6)$$

When assessing cyclone hazards in this way, it has to be borne in mind that the hazards obtained from the tracks simulated with an implementation of the model reflect only the average hazards over the whole time period considered. For example, the various modes of variability in cyclone activity explained in Holland (2007) are not considered separately from the rest of the data. Thus, the actual hazards in any given year may differ significantly from those obtained from the model. A possible way of dealing with this problem could be, instead of using all of the available data as input for the model, as it was done in the present study (see Section 1.3), to use only data from a period that exhibits similar values of certain influence factors as the time span for whose investigation the model is being applied. Such a period might be a selection of years with similar values of influence factors such as ENSO or AMO, which have their principal expression in sea surface temperatures (SST). Recall that SST are considered to be closely correlated to cyclone activity and intensity (i.e. wind speeds), see for example Mann and Emanuel (2006) or Holland and Webster (2007). More simply, one might also choose to consider a sequence of years with higher cyclone activity or higher counts in cyclone genesis. By selecting the input data in this way, the model should then reproduce the specific effects of these influences reflected in the data, consequently producing more accurate information about hazards in periods under investigation.

It is not clear, however, if this simple transfer of the model to different input data would be able to produce the desired results. While the transfer of the model itself does not pose an essential problem (the initial version of the model was applied to data from the western North Pacific, see Rumpf et al. (2007)), the selection of the input data would require extensive statistical investigations beyond the scope of this study. For example, this would mean a restriction to a potentially much smaller subset of the data, which could pose serious statistical difficulties, such as a heightened sensitivity of the results to outliers of any kind in the data. In addition, it would raise the question of how to separate the data appropriately: which years exactly are considered to be of 'high activity' and which ones are not? Furthermore, it would require a different data set as a basis, since ENSO, AMO, or SST are not included in HURDAT.

4 Simulation results

4.1 Simulation samples

The proposed model has been implemented in Java, in part using classes and methods from the GeoStoch library, see Mayer et al. (2004) and

http://www.geostoch.de . This implementation can be used to generate a dataset containing 100 times the number of storms found in the historical data within a few days on standard computers. Two examples of sets of synthetic storm tracks are shown in Figures 6 and 8. These figures show simulated tracks of class 1 and 2 cyclones, respectively. By juxtaposition with the historical class 1 tracks in Figure 5, it can be seen that the basic shapes and characteristics of the historical tracks are captured fairly well in the simulated class 1 tracks plotted in Figure 6. The same generally holds true for the sample of synthetic class 2 tracks (Figure 8) that have been juxtaposed with the historical tracks of class 2 storms (Figure 7), although the former tend to end somewhat earlier and curve northward slightly too far east compared with the latter.

4.2 Evaluation

In addition to the visual comparison between historical and synthetic storm tracks conducted in Section 4.1, a number of statistical comparisons are performed. These comparisons check the quality of the match between certain characteristics in the simulated data and the same characteristics in the entire historical data. The different modes of variability as stated in Holland (2007) (see also Section 3) are only considered indirectly through the fact that certain characteristics, such as for example the maximum wind speeds at certain locations, are influenced much more by certain values of theses modes, for example high SST, than others.

Initially, the numbers of storm tracks crossing certain zones of interest are counted for the historical dataset and for 100 samples of simulated storm tracks. Each sample covers the same time 106-year period as the historical data (see Section 1.3), i.e. it has been simulated with the same expected number of tropical cyclones. The zones chosen represent most of the areas with the highest relevance to the insurance industry, because on the one hand, they are known to be endangered by tropical cyclones and, on the other, they contain a significant amount of (potentially) insured values. The complete list of zones investigated is given in Table 1.

The results of the first part of this investigation are given in Table 1. This table lists the following values by zone: the number of historical storm tracks crossing that particular zone (x) and the sample mean ($\bar{x}_n$) and sample standard deviation (s_n) of that number in the 100 samples of simulated storm tracks. It is assumed that this number is normally distributed with a standard deviation given by s_n. Under the hypothesis that the expected number in real data is equal to $\bar{x}_n$, the value $z = \frac{x - \bar{x}_n}{s_n}$ is standard-normally distributed. The last column of the table indicates whether x is located within a certain interval around the simulated mean, i.e. if z is within the range $[-1.96, 1.96]$ where 1.96 is the 0.975-quantile of the standard normal

Number	Name	x	$\bar{x}_n$	s_n	TD
1	Bahamas	144	155.6	16.8	+
2	Barbados	29	26.3	5.3	+
3	Cayman	14	11.1	3.5	+
4	Dominican Republic	64	69.8	9.9	+
5	Florida	138	153.0	17.9	+
6	Houston/Galveston	48	46.0	7.3	+
7	Jamaica	24	28.3	5.1	+
8	New York	336	345.9	34.4	+
9	New Orleans	41	55.6	8.5	+
10	Puerto Rico	46	35.1	6.5	+
11	Yucatan	73	78.1	9.9	+

Table 1 Counts of storm tracks hitting zones of interest. Number: number of the zone of interest (as used in Tables 2 and 3); Name: name of the zone of interest; x: historical count; $\bar{x}_n$: simulated mean; s_n: simulated standard deviation; TD: test decision; +: hypothesis not rejected; −: hypothesis rejected.

distribution. This quantile was chosen such that the entries in the last column indicate the result of a standard Gaussian test at level $\alpha = 0.05$ of the above mentioned hypothesis. As can be seen from the table, this hypothesis is never rejected.

In addition to the frequencies of tropical cyclone landfalls in a certain zone, which are listed in Table 1, the so-called 'clash probabilities' are also of importance for insurers and reinsurers, i.e. the probabilities of a single cyclone hitting at least two zones of interest. The counts in the historical data and the simulated data for such events are shown in Table 2. The columns are used in analogy to those in Table 1. Again, the table shows a good agreement between the historical and the simulated data, the two exceptions being cyclones that strike the Bahamas and Yucatan and those which make landfall in Barbados and Puerto Rico.

Investigation of the model's performance also focuses on simulated wind speeds in the regions of interest. Table 3 shows the counts of points of measurement of tropical cyclones where winds reach hurricane intensity. The meaning of the columns is the same as in Tables 1 and 2. Category 1-3 and category 4-5 hurricanes are investigated separately. It can be seen that the agreement between historical and simulated data is decent with the exception of category 1-3 hurricanes making landfall in the Bahamas, although the variability in the simulated data appears relatively high for some zones.

The last step in the comparison between historical and simulated data consists of a selection of so-called 'two-sample-goodness-of-fit tests', a kind of statistical hypothesis tests used to check whether the distribution functions of two random samples which are considered to consist of independent

Z	x	$\bar{x}_n$	s_n	TD	Z	x	$\bar{x}_n$	s_n	TD
1, 2	1	2.0	1.3	+	4, 5	10	12.5	3.1	+
1, 3	3	2.8	1.6	+	4, 6	2	1.8	1.4	+
1, 4	15	21.3	5.2	+	4, 7	5	6.8	2.5	+
1, 5	61	61.6	9.7	+	4, 8	22	32.8	6.5	+
1, 6	2	6.1	2.6	+	4, 9	1	2.7	1.6	+
1, 7	6	4.5	2.1	+	4, 10	24	19.9	4.5	+
1, 8	75	95.1	13.1	+	4, 11	5	8.2	2.8	+
1, 9	8	11.6	3.5	+	5, 6	6	8.0	3.5	+
1, 10	11	11.8	3.3	+	5, 7	3	3.4	1.7	+
1, 11	4	10.2	3.0	−	5, 8	84	98.2	13.6	+
2, 3	0	0.6	0.8	+	5, 9	19	22.2	5.0	+
2, 4	3	3.0	1.6	+	5, 10	8	6.5	2.6	+
2, 5	2	2.0	1.5	+	5, 11	5	8.6	3.0	+
2, 6	0	0.4	0.7	+	6, 7	0	0.7	0.8	+
2, 7	1	1.6	1.2	+	6, 8	23	17.5	4.6	+
2, 8	4	5.7	2.6	+	6, 9	15	15.9	4.3	+
2, 9	1	0.4	0.7	+	6, 10	1	0.9	1.1	+
2, 10	6	1.5	1.2	−	6, 11	6	3.4	1.9	+
2, 11	0	3.0	1.7	+	7, 8	10	12.3	3.4	+
3, 4	0	2.8	1.7	+	7, 9	0	0.7	0.8	+
3, 5	3	1.4	1.2	+	7, 10	3	2.0	1.2	+
3, 6	0	0.5	0.7	+	7, 11	9	6.0	2.2	+
3, 7	5	2.9	1.7	+	8, 9	25	30.2	6.1	+
3, 8	8	4.6	2.4	+	8, 10	16	13.7	3.9	+
3, 9	0	0.4	0.6	+	8, 11	23	21.3	5.8	+
3, 10	0	0.9	1.0	+	9, 10	1	1.4	1.2	+
3, 11	6	3.7	2.1	+	9, 11	4	3.2	2.0	+
					10, 11	4	3.0	1.6	+

Table 2 Numbers of storm tracks hitting two zones of interest. Z: Zones of interest (see Table 1); x: historical count; $\bar{x}_n$: simulated mean; s_n: simulated standard deviation; TD: test decision; +: hypothesis not rejected; −: hypothesis rejected.

and identically distributed sample variables agree (for details on hypothesis testing, see, for example, Lehmann and Romano (2005)). For this purpose, wind impacts (see Section 3) at 7,182 specific locations within the zones of interest (see Table 1) were calculated for the historical as well as for the simulated data. In this way, two samples, a historical one with distribution function F_{hist}, and a simulated one with distribution function F_{sim}, were created for each of the 7,182 locations. If the historical data is represented well by the simulated data, the samples of wind impacts from the two datasets at one and the same location should be very similar, i.e. they should have the same underlying distribution function. Therefore, three different tests of the hypothesis that the distribution functions of these two samples are the same, i.e.

$$H_0 : F_{hist}(x) = F_{sim}(x) \ \forall x \in \mathbb{R} \ , \tag{7}$$

Z	C	x	$\bar{x}_n$	s_n	TD	Z	C	x	$\bar{x}_n$	s_n	TD
1	1-3	55	2	26.7	−	1	4-5	53	62.8	22.0	+
2	1-3	0	1.8	2.8	+	2	4-5	0	0.7	1.2	+
3	1-3	0	1.3	2.3	+	3	4-5	1	1.1	1.5	+
4	1-3	16	15.7	6.2	+	4	4-5	2	8.1	4.7	+
5	1-3	104	142.7	19.8	+	5	4-5	25	52.3	14.8	+
6	1-3	90	63.6	16.1	+	6	4-5	18	18.0	8.4	+
7	1-3	5	14.1	9.4	+	7	4-5	3	9.1	9.2	+
8	1-3	11	7.4	4.8	+	8	4-5	1	1.0	1.5	+
9	1-3	67	56.2	15.6	+	9	4-5	17	12.3	5.4	+
10	1-3	6	7.2	5.0	+	10	4-5	3	2.3	3.2	+
11	1-3	72	88.9	24.2	+	11	4-5	15	33.5	19.4	+

Table 3 Points of measurement of hurricanes of different categories in the different zones. Z: Zone of interest (see Table 1); C: Categories of hurricanes; x: historical count; $\bar{x}_n$: simulated mean; s_n: simulated standard deviation; TD: test decision; +: hypothesis not rejected; −: hypothesis rejected.

were performed for each location. The following tests were used:

− Kolmogorov-Smirnov test (KST). This test checks H_0 against the general alternative that the values of the two distribution functions differ for some $x \in \mathbb{R}$. That means that any differences between the two samples will lead to the rejection of H_0 if they are too large in the statistical sense, regardless of the wind impacts at which these differences might occur. For mathematical details, see, for example, Gibbons (1985), p. 127ff.

− Wilcoxon rank test (WRT). This test is especially sensitive to deviations in the location parameters of F_{hist} and F_{sim}, i.e. it is used to determine whether one of the distribution functions is shifted relative to the other. Thus, differences in variabilities of wind impacts within the two samples will not lead to the rejection of H_0 as easily as differences in the means or medians of the two samples. For mathematical details, see, for example, Gibbons (1985), p. 164ff., or Lehmann and Romano (2005), p.243.

− Ansari-Bradley test (ABT). In contrast to the WRT, the ABT detects differences in scale between F_{hist} and F_{sim}. Thus, it is used to check H_0 against the alternative that F_{hist} is a scaled version of F_{sim} (or vice versa). In other words: while differences in the means or medians of the two samples of wind impacts are considered more tolerable, differences in the variabilites will lead to the rejection of H_0 by this test more easily. For mathematical details, see, for example, Gibbons (1985), p. 179ff.

All the two-sample-goodness-of-fit tests were performed using methods available in version 2.3.1 of the R programming language (see R Development Core Team (2006)).

The numbers of points (out of 7,182) for which H_0 was rejected by the three tests at different levels of significance α are listed in Table 4. The

column marked 'All' indicates the number of points where H_0 was rejected by all three tests, whilst the last column in contrast contains the number of points where none of the tests rejected H_0. A closer look at the locations where the hypothesis of equal distribution functions was rejected by all tests shows that, at those points, the average wind speeds and the variance in wind speeds appear to have been underestimated. Most are situated off the coast of New York. One possible interpretation of this might be that class 2 storms, i.e. the class which contains storms recurring from a western to a northeastern bearing and affecting the eastern part of the North American continent (see Section 2.1 and Rumpf et al. (2007)), are not simulated in the model with the requisite precision. Most of the other cyclone tracks seem to be represented very well. The fit seems especially good in the Caribbean and in and around the Gulf of Mexico.

Note that it is not appropriate to draw any conclusions from a comparison of the relative rejection frequencies given in Table 4 to the respective levels of significance, i.e. the probabilities of type I errors, since the wind speed distributions at different locations have been derived from the same data and are therefore strongly dependent.

α	KST	WRT	ABT	All	None
0.01	229	219	261	45	6,632
0.05	1,018	785	989	244	5,138
0.10	1,575	1,559	1,794	562	4,083

Table 4 Numbers of points where H_0 was rejected by the different tests

5 Summary and outlook

A model for the Monte-Carlo simulation of tropical cyclone tracks has been enhanced and applied to historical data from the North Atlantic Ocean basin in order to improve tropical cyclone hazard assessment. The simulation of a large number of tracks with an implementation of this model now allows for a calculation of a large number of 'wind impacts' at any location of interest affected by tropical cyclones. The resulting large numbers of wind impacts can be used to estimate the expected return periods of certain wind speeds. This, in turn, makes it possible to estimate the expected damages and other characteristics of interest to the insurance and reinsurance industry.

In the present study, the model was applied to the complete historical data from 1900-2005. For the investigation of the effects of certain influence factors, such as those stated in Holland (2007), some extensive statistical

investigations of the corresponding subsets of data would have to be performed, which will be the subject of future research. Especially when aiming to include potential effects of climate change, such as trends in SST, a careful scrutiny of the input data is necessary, since the model is in large parts data-driven. Thus, the fact that for example certain levels of SST values may not have been observed in the historical data would create a need for extrapolation of the data. Possible effects of these modes of variability and trends might for example be changes in the structure of the point patterns formed by the points of tropical cyclone genesis (and resulting changes in proportions or shapes of the six different storm classes), as well as changes in cyclone frequencies or the distribution of wind speeds, which all could potentially result in differences in the hazards obtained from the model.

Acknowledgements

References

Baddeley A, Gregori P, Mateu J, Stoica R, Stoyan D (eds.) (2006) Case Studies in Spatial Point Process Modeling. Lecture Notes in Statistics 185. Springer, New York

Baddeley A, Turner R (2005) `spatstat`: an `R` package for analyzing spatial point patterns. J. Stat. Softw. 12 (6): 1–42.
URL: http://www.jstatsoft.org

Demuth J, DeMaria M, Knaff JA (2006) Improvement of advanced microwave sounder unit tropical cyclone intensity and size estimation algorithms. J. Appl. Meteor. 45, 1573–1581.

Diggle PJ (2003) Statistical Analysis of Spatial Point Patterns. 2nd Edition. Arnold, London

Emanuel KA, Ravela S, Vivant E, Risi C (2006) A statistical deterministic approach to hurricane risk assessment. B. Am. Meteorol. Soc. 87: 299–314

Gibbons JD (1985) Nonparametric Statistical Inference. 2nd edition. Marcel Dekker, New York

Hall TM, Jewson S (2007) Statistical modeling of North Atlantic tropical cyclone tracks. Tellus, 59A, 486–498

Holland GJ (1980) An analytic model of the wind and pressure profiles in hurricanes. Mon. Weather Rev. 108: 1212–1218

Holland GJ (2007) Misuse of landfall as a proxy for Atlantic tropical cyclone activity. EOS Trans. Am. Geophys. Union 88 (36), 349–350

Holland GJ, Webster PJ (2007) Heightened tropical cyclone activity in the North Atlantic: Natural variability or climate trend? Philos. Trans. R. Soc. London, Ser. A, 365 (1860), 2695–2716

Iman RL, Johnson ME, Watson CC (2006) Statistical aspects of forecasting and planning for hurricanes. The American Statistician 60 (2): 105–121

Jarvinen BR, Neumann CJ, Davis MAS (1984) A tropical cyclone data tape for the north Atlantic basin, 1886-1983, contents, limitations and uses. NOAA Tech. Memo., NWS NHC 22, Miami, FL

Lehmann EL, Romano JP (2005) Testing Statistical Hypotheses. 3rd edition. Springer, New York

Mann ME, Emanuel KA (2006) Atlantic hurricane trends linked to climate change. EOS Trans. Am. Geophys. Union 87 (24), p. 233, 238, 241

Mayer J, Schmidt V, Schweiggert F (2004) A unified simulation framework for spatial stochastic models. Simul. Model. Pract. Th. 12: 307–326

Meyn SP, Tweedie RL (1993) Markov Chains and Stochastic Stability. Springer, London

Munich Reinsurance Company (2006) Hurricanes - More intense, more frequent, more expensive. Insurance in a time of changing risks. Munich, Germany.
URL: http://www.munichre.com/publications/302-04891_en.pdf

R Development Core Team (2006) R: A language and environment for statistical computing. R Foundation for Statistical Computing, Vienna, Austria

Rumpf J, Rauch E, Schmidt V, Weindl H (2006) Stochastic modeling of tropical cyclone track data. 27th Conference on Hurricanes and Tropical Meteorology, April 24–28, 2006, Monterey, CA

Rumpf J, Weindl H, Höppe P, Rauch E, Schmidt V (2007) Stochastic modelling of tropical cyclone tracks. Math. Meth. Oper. Res., 66 (3), 475–490

Silverman BW (1986) Density Estimation for Statistics and Data Analysis. Chapman & Hall, New York

Stoyan D, Stoyan H (1994) Fractals, Random Shapes and Point Fields. Methods of Geometrical Statistics. J. Wiley & Sons, Chichester

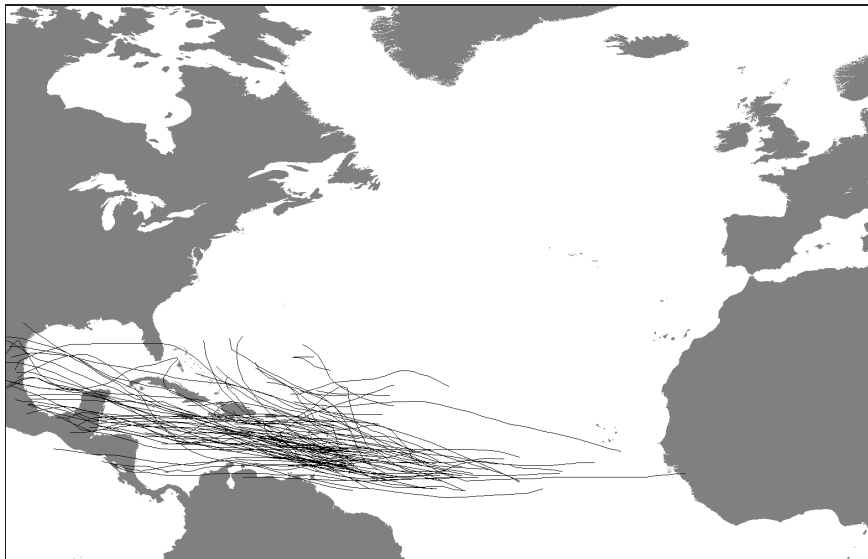Stroock DW (2005) An Introduction to Markov Processes. Springer, Berlin

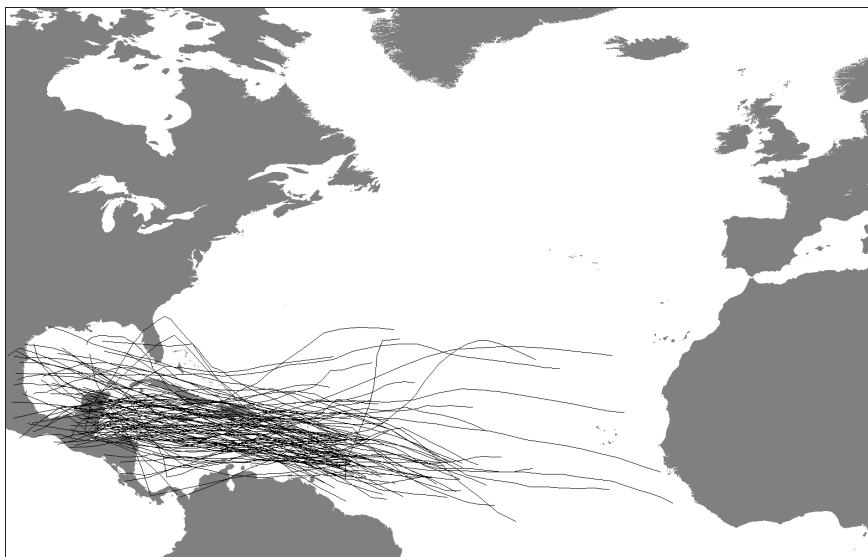**Figure 5** Tracks of historical class 1 storms

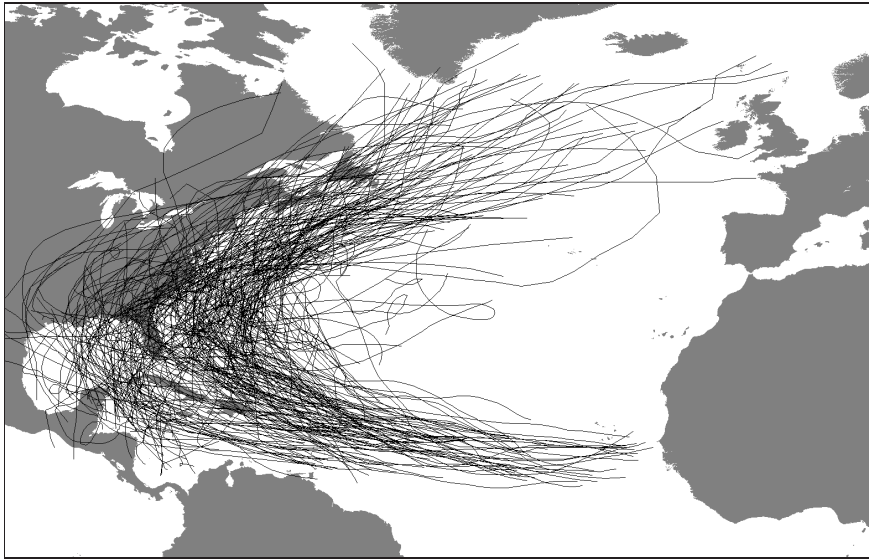**Figure 6** Tracks of a sample of simulated class 1 storms
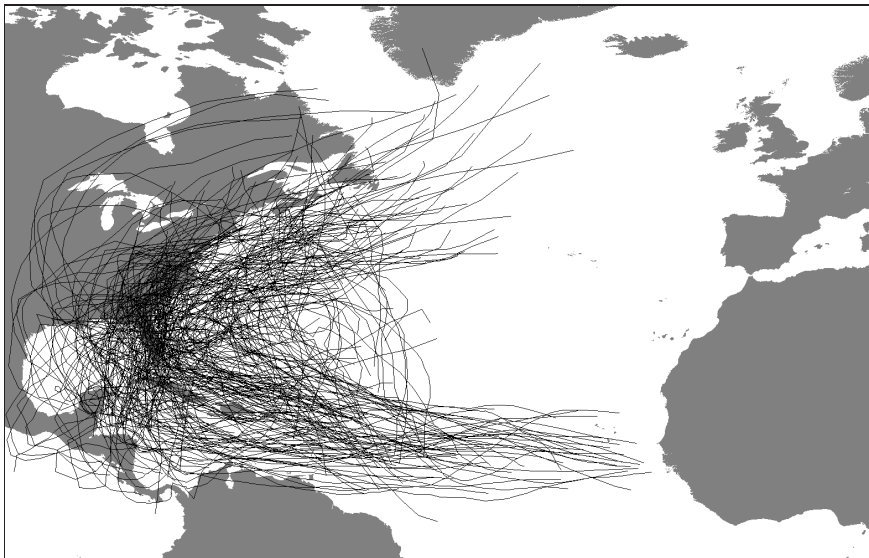
Figure 7 Tracks of historical class 2 storms

Figure 8 Tracks of a sample of simulated class 2 storms